Self-Assembly

DOI: 10.1002/anie.201006681

Cooperative Assembly of Binary Molecular Components into Tubular Structures for Multiple Photonic Applications**

Qing Liao, Hongbing Fu, Chen Wang, and Jiannian Yao**

One-dimensional (1D) assemblies of π-stacked conjugated molecules are of particular interest for miniaturized electronic[1] and photonic[2] devices. Inspired by the discovery of carbon nanotubes, hollow tubular structures been intensively investigated in the past decades.[3] Research into organic tubes, however, has been slower than that of their inorganic counterparts. Supramolecular nanotube architectures of amphiphilic molecules[4a] and peptides[4b] have been constructed by a twisted-belt mechanism, while the template-wetting method has been developed for the preparation of polymer nanotubes.[5] Nonetheless, the self-assembly of tubular structures from π-conjugated molecules,[6] especially from multiple molecular components, remains largely unexplored.

The cooperative assembly of multiple π-conjugated components has been recently introduced as an effective approach to the fabrication of photo- and/or electroactive nanostructures,[7] in which adjustable electronic processes, such as electron transfer and energy transfer, between different species allow the realization of novel properties, such as p/n heterojunctions,[8a] ambipolar charge transport,[8b] and white-light emission.[9] Herein, we report a supramolecular synthesis of rectangular binary microtubes with precisely controlled lengths by cooperative assembly of 2,4,5-triphenylimidazole (TPI, a ultraviolet-emissive molecule) and 3-(anthracen-10-yl)-1-phenylpro-2-en-1-one (APO, a green-emissive and photoactive molecule; Figure 1a). In contrast to the orthogonal self-assembly that takes place at room temperature, the cooperative assembly of TPI and APO mediated by hydrogen bonding has been achieved at 65 °C, and leads to 1D growth of homogeneous tubular structures. As a result of their well-defined facets, rectangular binary tubes behave as annular microcavities that are capable of propagating both TPI and APO photoluminescence (PL). Furthermore, the controllable switching of guided light to a selected end of a single tube has been demonstrated by the photoisomerization of APO molecules that was induced locally upon focused light irradiation.

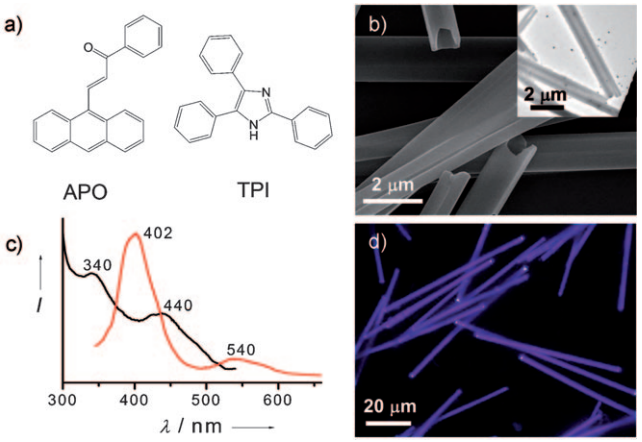

Figure 1. a) Molecular structures of APO and TPI. b) SEM and TEM (inset) images of as-prepared binary microtubes. c) Normalized diffuse reflection absorption (black) and PL (red, $\lambda_{EX} = 320$ nm) spectra of an ensemble of binary tubes placed on a quartz substrate. d) PL micrograph of binary microtubes on a quartz substrate upon excitation with unfocused UV light (330–380 nm).

In a typical preparation, a mixed stock solution (100 μL) containing both TPI (1 mM) and APO (1 mM) in tetrahydrofuran (THF) was rapidly injected into deionized water (2 mL) at 65 °C under shaking. The mixture was maintained at 65 °C for 30 min, and then the hot mixture was slowly cooled to 25 °C at a rate of 10 °C h^{-1}. Finally, the precipitates were centrifugally separated from the colloidal suspension and washed twice with water prior to vacuum drying.

Scanning electron microscopy (SEM) results (Figure 1b) reveal that highly monodispersed 1D structures with a rectangular cross-section were obtained. The open-end features suggest that the structures are rectangular hollow tubes with a wall thickness of approximately 200 nm. These results are further supported by transmission electron microscopy (TEM) analysis (Figure 1b, inset). Each individual tube has a uniform diameter around 800 nm and smooth outer surfaces along the entire length (60 μm; Figure S1 in the Supporting Information). Moreover, the well-defined facets of these tubes are also confirmed by atomic force microscopy (AFM) measurements (Figure S2).

Figure 1c shows the diffuse reflection absorption (black) and PL spectra (red) of an ensemble of tubes placed on a quartz plate. Two evident absorption peaks at 340 and 440 nm are observed. The former is due to the $S_0 \rightarrow S_1$ transition of the TPI molecules,[10a] and the latter is a characteristic of the APO components (Figure S3).[10b] Moreover, besides the TPI band

[*] Dr. Q. Liao, Prof. H. B. Fu, C. Wang, Prof. J. N. Yao
Beijing National Laboratory for Molecular Science (BNLMS)
Institute of Chemistry, Chinese Academy of Sciences
Beijing, 100190 (P. R. China)
E-mail: hongbing.fu@iccas.ac.cn
jnyao@iccas.ac.cn

[**] This work was supported by grants-in-aid from the Natural Science Foundation of China (nos. 90301010, 20873163, 20803085, 20925309), the Chinese Academy of Sciences ("100 Talents" program), and the National Research Fund for Fundamental Key Project 973 (2011CB808402).

Supporting information for this article is available on the WWW under http://dx.doi.org/10.1002/anie.201006681.

at 402 nm, the PL spectrum of tubes excited at 320 nm also exhibits the PL of APO at 540 nm. Note that APO components only weakly absorb light at 320 nm (Figure S3). Considering the good spectral overlap between the TPI emission and the APO absorption (Figure S3), the APO PL observed for binary tubes upon excitation at 320 nm might be a result of Förster energy transfer (FET) from excited TPI to APO molecules.[11] Indeed, the decay of TPI PL in binary tubes (109 ps) is faster than that in pure TPI microrods (301 ps), and results in an FET efficiency of 0.64 (Figure S4).

According to the absorption analysis of binary tubes re-dissolved in THF, the contents of TPI and APO are determined to be $(92\pm3)\%$ and $(8\pm2)\%$, respectively (Figure S5). Figure 1d shows the PL micrograph of binary tubes excited with unfocused UV light (330–380 nm). Blue-violet PL occurs uniformly along the tube bodies with bright white spots at both ends. The spatially resolved PL spectra indicate that the intensity fluctuation across the entire spectral region is less than 10% at different positions for a single tube (Figure S6). Furthermore, X-ray diffraction (XRD) results suggest that binary tubes are highly crystalline, however, this property is mainly related to the TPI component (Figure S7). In fact, no XRD characteristics of APO component were identified. It is known that besides the spectral overlap, the FET process also requires a close distance of about 2–6 nm between the donor and acceptor molecules.[11] Therefore, the frustrated FET process (efficiency = 0.64) suggests that the APO molecules are distributed between small crystal grains of TPI matrix in binary microtubes, which are different from the common molecular dispersed film doping, where the donor PL can be completely quenched.

Individual TPI and APO molecules can self-assemble into solid microrods by π stacking at 25 °C (Figure S8); consequently, orthogonal assembly takes place if the mixed solution is applied (Figure S9). By raising the temperature to 65 °C, individual TPI or APO molecules form irregular particles (Figure S10); remarkably, cooperative self-assembly generates rectangular binary tubes. Figure 2a shows the IR spectra of binary tubes, individual TPI, and APO solid rods, and the following can be observed: 1) the peaks at 3416 cm^{-1} of N–H stretching observed in TPI rods red-shift to 3349 cm^{-1} and become broader and stronger in the binary tubes; 2) the peaks at 1597 (C=C stretching) and 1656 cm^{-1} (C=O stretching) observed in APO rods become weaker in the binary tubes; and 3) unsaturated C–H stretching at 3052 cm^{-1} occurs in both TPI and APO rods; however, saturated C–H stretching at 2904 cm^{-1} occurs concurrently with the appearance of a broad feature around 1050 cm^{-1} typical for C–O stretching in binary tubes. All these features suggest the existence of intermolecular hydrogen bonding between the N–H of TPI and C=O of APO in binary tubes.

Temporal SEM analysis was employed to further probe the formation process of binary tubes (Figure 2c–f). We have identified three distinctive stages: nucleating aggregation, 1D growth, and termination (Figure 2b). At an early stage about 2 min after the injection, short and round hollow structures are already observed with a diameter of 350 nm and a length of 3 μm (Figure 2c). These initial hollow structures undergo a

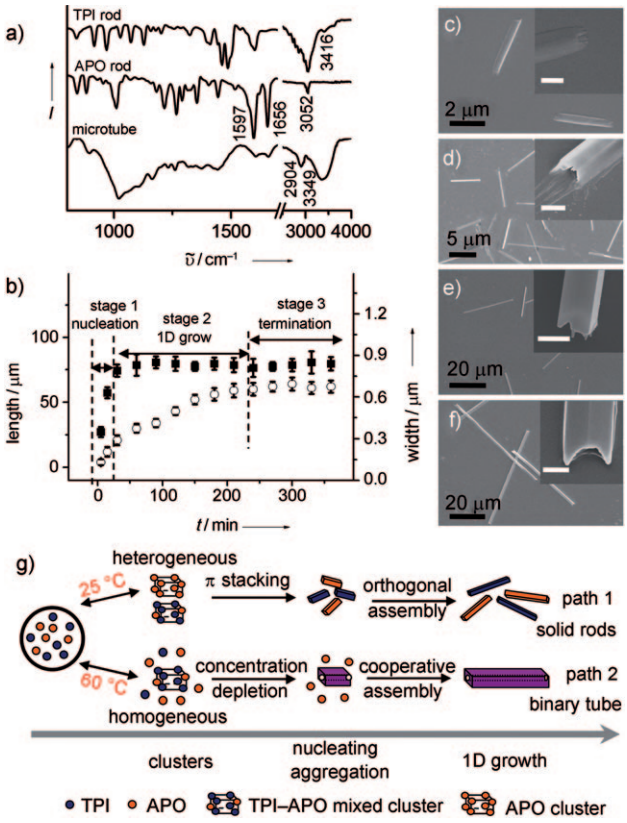

Figure 2. a) Infrared spectra of the TPI rods (top), APO rods (middle), and binary tubes (bottom). b) Length (hollow circle) and diameter (solid square) of microtubes plotted as a function of reaction time, based on SEM analysis of binary microtubes obtained at different reaction intervals c) 2 min, d) 10 min, e) 1 h, and f) 3 h. The insets show corresponding high-magnification SEM images. The scale bars represent 1 μm. g) A schematic model of cooperative self-assembly for the formation of binary tubular structures.

rapid growth that results in rectangular tubes with a diameter of 650 nm and a length of 12 μm at 10 min (Figure 2d). Further prolongation of the reaction time to longer than 10 min leads to the 1D growth stage. In this stage (Figure 2b), the tube diameter remains almost constant around 800 nm; however, the tube length keeps growing as the reaction time is increased, for example, the length is 30 μm after 1 h (Figure 2e) and 60 μm after 3 h (Figure 2f). After the reaction time exceeds 3 h, both the transverse and longitudinal growth terminate (Figure 2b). The formation of binary tubes follows a typical 1D growth process rather than the twisted-belt mechanism reported for amphiphilic molecules and peptides,[4] or the recently reported "etching" mechanism,[12] in which crystalline tubular structures are converted from their solid counterparts by dissolution using either liquid or gaseous solvents.

Most recently, Jonkheijm et al. demonstrated a close relationship between the self-assembly process and the nucleation–growth pathway, where self-assembled molecular clusters are identified as a high-energy prenucleus.[13] In our case, the TPI and APO components can be selectively excited at 320 and 440 nm, respectively. At room temperature, we found that the dilute mixed solution ($\leq 4.0\times10^{-5}$ M) shows

only the PL of TPI upon excitation at 320 nm (Figure S11a), because both the TPI and the APO molecules are separately free-standing. In contrast, the PL of APO is dominant in the PL spectrum of the stronger stock solution (1 mM) excited at 320 nm, thus suggesting the exclusive formation of TPI–APO mixed clusters (Figure S11a), in which the spatial proximity between TPI and APO molecules ensures the FET process. Upon selective excitation of APO at 440 nm (Figure S11b), observation of a severe concentration quenching effect ($> 3.0\times10^{-4}$ M) confirms that APO clusters are also formed in the stock solution.[14] Most importantly, if the stock solution is heated to 65 °C, the fluorescence signal of APO PL excited at 440 nm reappers with an intensity three times that recorded at 25 °C, probably because of the dissociation of APO clusters. Meanwhile, the PL spectrum excited at 320 nm (Figure S11) indicates that despite the dissociation, some of TPI–APO mixed clusters remained intact at 65 °C.

By combining the above results, we propose a cooperative assembly model for the formation of binary tubes in Figure 2g. Upon injection, the solvent exchange induces the nucleation event. At room temperature (path 1), both TPI–APO mixed clusters and APO clusters can serve as nuclei for heterogeneous assembly driven by the π-stacking motif of TPI or APO molecules. Therefore, orthogonal self-assembly takes place, and leads to TPI and APO solid rods (path 1). At 65 °C (path 2), the APO clusters are dissociated; only TPI–APO mixed clusters survive as high-energy nuclei for further homogeneous cooperative assembly. In the presence of APO monomers in the hot system, those APO molecules incorporated at the periphery of mixed clusters might dynamically exchange on (formation) and off (dissociation) the mixed clusters,[15] thus serving as a linker for aggregation of mixed clusters by hydrogen-bonding during the nucleation process. Although it is not yet fully understood, the aggregation of nucleates might cause temporary concentration depletion, which is responsible for the formation of primary hollow structures (path 2).[16] Once initial hollow structures form, 1D growth is energetically favorable because of the preferable adsorption of the growth units of the mixed clusters on the edge of primary tubular structures (path 2).[17] Note that the system was maintained at 65 °C for 30 min after the injection, and then the system was slowly cooled down at a rate of 10 °C h^{-1}. In the first 150 min (52 μm long tubes were obtained as shown in Figure 2b), the temperature is higher than 45 °C. Therefore, the TPI–APO mixed clusters play a major role in both the nucleation and growth processes. The solution that remains after the centrifugation shows only the absorption characteristics of APO (nanoparticles according to SEM), thus suggesting that all the TPI molecules are involved in tube formation. We also monitored the growth process by measuring the PL spectra excited at 320 nm. It is found that the ratio between the PL intensities of APO and TPI, I_{APO}/I_{TPI}, increases as the reaction time is extended (Figure S12). The variation of I_{APO}/I_{TPI} with time correlates well with that of the tube length versus time (circles in Figure 2b), thus verifying the incorporation of APO in the 1D tube growth.

As shown in Figure 1d, these binary microtubes present typical features of an active waveguide, such as bright PL spots at the tips and weaker emission from the bodies.[3] Propagation loss measurements were performed based on the spatially resolved PL spectra of a single tube by collecting the PL signal from one of its ends with respect to the distance travelled (Figure 3a). According to the equation of the

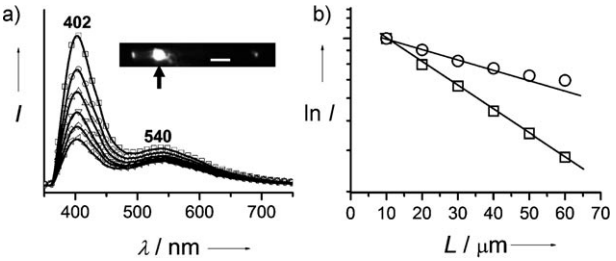

Figure 3. a) Spatially resolved PL spectra of out-coupled light at a distance of 10, 20, 30, 40, 50, and 60 μm (curves from top to bottom) from the tip of a single tube, recorded by focused 325 nm laser excitation (see the arrow in the inset). The scale bar is 10 μm. b) Logarithmic plot of the relative PL intensities at 402 nm (square) and 540 nm (circle) versus the propagation distance.

optical loss coefficient of guided light in the fundamental modes of a waveguide [Eq. (1)]:[12c]

$$\alpha = -10\log(I_{out}/I_{in})\,L^{-1} \quad (1)$$

where I_{in} and I_{out} are the intensities of incidence and out-coupled light, respectively, and L is the propagation distance, the values of α for TPI PL at 402 nm and for APO PL at 540 nm are determined to be 100 and 36 dB mm^{-1}, respectively (Figure 3b). It has been established that the air medium inside the tubes that have well-defined facets leads to spatial confinement of guided photons in two dimensions in the thin tubular wall, thereby forming an annular microcavity.[12b,c] The travel distance of the guided light in the annular microcavity is so long that a photon in the UV region from TPI can be reabsorbed by APO, which then re-emits a photon in the green region. This so-called remote energy relay (RER) process results in re-distribution of the guided PL from short to long wavelengths,[12c] and is the reason why the value of α at 540 nm is much lower than that at 402 nm.

The chalcone derivatives such as APO are photochemically active, and might undergo either photoisomerization or photodimerization.[18] We found that the green fluorescence of an ensemble of APO microrods placed on a quartz plate can be quenched by exposure to light (UV_{400}) from an Hg lamp equipped with a band-pass filter (central wavelength: 400 nm, FWHM: 40 nm), probably because of the photoisomerization reaction.[18a] The reversible recovery of green fluorescence can be easily achieved by keeping the irradiated sample in the dark (Figure S13). Figure 4a shows a schematic picture of a waveguide switch based on binary microtubes. Snapshots during the waveguide switch measurement are presented in Figure S14. Photoisomerization of APO components is induced locally by focusing 400 nm light from the Hg lamp down to the diffraction limit (2 μm) on a selected position on the tube, as indicated by the circle in Figure 4a. According to the spatially resolved spectra at the irradiation

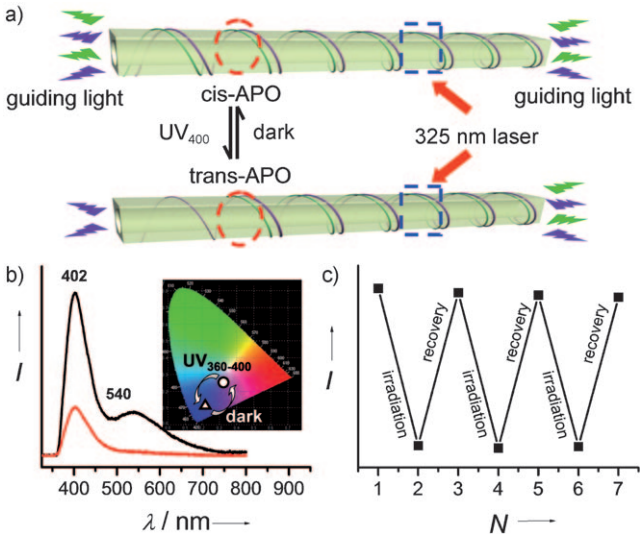

Figure 4. a) Representation of waveguide switch before (top) and after (bottom) irradiation of the region marked with a circle by UV_{400} light (FWHM: 40 nm). The squares show the excitation point of focused 325 nm laser light for waveguide measurement. b) Out-coupled PL spectra from the left tip before (black) and after (red) UV_{400} irradiation at the region marked with a circle, upon excitation at 325 nm by focusing the laser on the region marked with a square. c) The switch cycles (N = number of cycles) of APO PL out-coupled at the left tip upon UV_{400} irradiation at the circled region and subsequent recovery in the dark.

point (Figure S14d), the PL of TPI remain the same as that before irradiation, while the PL from APO is indeed quenched. We next checked the effect of UV_{400} irradiation at the circled region on the waveguide behavior by excitation at the region indicated by a square by using focused 325 nm laser light (Figure 4a). Figure 4b shows the out-coupled spectra collected at the left tip. The intensity of TPI PL after UV_{400} irradiation is about one-third of that before irradiation. Moreover, the PL of APO out-coupled at the left tip disappears completely after UV_{400} irradiation at the circled region. The inset of Figure 4b shows the CIE coordinates calculated from the out-coupled PL spectra at the left tip before (line 1) and after UV_{400} irradiation (line 2). In sharp contrast, the out-coupled spectra at the right tip show no changes in both TPI and APO features. That is, selective switching of the waveguide to the left tip had been successfully realized by using our binary tube.[19] Remarkably, the APO PL out-coupled at the left tip can be turned on again by keeping the irradiated sample in the dark. This switch has an on/off ratio of approximately 20 and can be reversibly switched over at least seven cycles without any fatigue (Figure 4c).

In summary, we have reported the preparation of rectangular binary microtubes with precisely controlled lengths through cooperative self-assembly of TPI and APO. We have identified three stages of the formation binary tubes: nucleating aggregation, 1D growth, and termination. In particular, TPI–APO mixed clusters play a major role in the cooperative self-assembly for the nucleation and growth of binary tubes. These microtubes behave as annular microcavities that are capable of propagating both TPI and APO PL along the 1D direction. Furthermore, the controllable switching of guided light to a selected end of a single tube has been demonstrated by local introduction of photoisomerization of APO component upon focused light irradiation. The strategy described here might be useful for the design and fabrication of novel optoelectronic devices.

Received: October 25, 2010
Revised: February 18, 2011

Keywords: π conjugation · energy transfer · microtubes · photonics · self-assembly

[1] a) H. Moon, R. Zeis, E. J. Borkent, C. Besnard, A. J. Lovinger, T. Siegrist, C. Kloc, Z. N. Bao, *J. Am. Chem. Soc.* **2004**, *126*, 15322–15323; b) L. Zang, Y. Che, J. Moore, *Acc. Chem. Res.* **2008**, *41*, 1596–1608.

[2] a) Y. S. Zhao, H. B. Fu, A. D. Peng, Y. Ma, Q. Liao, J. N. Yao, *Acc. Chem. Res.* **2010**, *43*, 409–418; b) D. O'Carroll, I. Lieberwirth, G. Redmond, *Nat. Nanotechnol.* **2007**, *2*, 180–184.

[3] a) J. Hu, M. Ouyang, P. Yang, C. M. Lieber, *Nature* **1999**, *399*, 48–51; b) J. P. Hill, W. Jin, A. Kosaka, T. Fukushima, H. Ichihara, T. Shimomura, K. Ito, T. Hashizume, N. Ishii, T. Aida, *Science* **2004**, *304*, 1481–1483; c) A. N. Aleshin, *Adv. Mater.* **2006**, *18*, 17–27; d) Y. S. Zhao, W. S. Yang, D. B. Xiao, X. H. Sheng, X. Yang, Z. G. Shuai, Y. Luo, J. N. Yao, *Chem. Mater.* **2005**, *17*, 6430–6435.

[4] a) T. Shimizu, M. Masuda, H. Minamikawa, *Chem. Rev.* **2005**, *105*, 1401–1443; b) D. T. Bong, T. D. Clark, J. R. Granja, M. R. Ghadiri, *Angew. Chem.* **2001**, *113*, 1016–1041; *Angew. Chem. Int. Ed.* **2001**, *40*, 988–1011.

[5] M. Steinhart, R. B. Wehrspohn, U. Gösele, J. H. Wendorff, *Angew. Chem.* **2004**, *116*, 1356–1367; *Angew. Chem. Int. Ed.* **2004**, *43*, 1334–1344.

[6] a) Z. C. Wang, C. J. Medforth, J. A. Shelnutt, *J. Am. Chem. Soc.* **2004**, *126*, 15954–15955; b) J. S. Hu, Y. G. Guo, H. P. Liang, L. J. Wan, L. Jiang, *J. Am. Chem. Soc.* **2005**, *127*, 17090–17095; c) Y. Chen, B. Zhu, F. Zhang, Y. Han, Z. Bo, *Angew. Chem.* **2008**, *120*, 6104–6107; *Angew. Chem. Int. Ed.* **2008**, *47*, 6015–6018.

[7] F. J. M. Hoeben, P. Jonkheijm, E. W. Meijer, A. P. H. J. Schenning, *Chem. Rev.* **2005**, *105*, 1491–1546.

[8] a) N. Sakai, R. Bhosale, D. Emery, J. Mareda, S. Matile, *J. Am. Chem. Soc.* **2010**, *132*, 6923–6925; b) P. Jonkheijm, N. Stutzmann, Z. J. Chen, D. M. de Leeuw, E. W. Meijer, A. P. H. J. Schenning, F. Würthner, *J. Am. Chem. Soc.* **2006**, *128*, 9535–9540.

[9] a) C. Vijayakumar, V. K. Praveen, A. Ajayaghosh, *Adv. Mater.* **2009**, *21*, 2059–2063; b) R. Abbel, C. Grenier, M. J. Pouderoijen, J. W. Stouwdam, P. E. L. G. Leclère, R. P. Sijbesma, E. W. Meijer, A. P. H. J. Schenning, *J. Am. Chem. Soc.* **2009**, *131*, 833–843; c) Y. L. Lei, Q. Liao, H. B. Fu, J. N. Yao, *J. Am. Chem. Soc.* **2010**, *132*, 1742–1743.

[10] a) Y. S. Zhao, A. D. Peng, H. B. Fu, Y. Ma, J. N. Yao, *Adv. Mater.* **2008**, *20*, 1661–1665; b) H. D. Becker, K. Andersson, *J. Org. Chem.* **1983**, *48*, 4542–4549.

[11] J. R. Lakowicz, *Principles of Fluorescence Spectroscopy*, Plenum, New York, **1999**.

[12] a) X. J. Zhang, X. H. Zhang, W. S. Shi, X. M. Meng, C. S. Lee, S. T. Lee, *Angew. Chem.* **2007**, *119*, 1547–1550; *Angew. Chem. Int. Ed.* **2007**, *46*, 1525–1528; b) Y. S. Zhao, J. J. Xu, A. D. Peng, H. B. Fu, Y. Ma, L. Jiang, J. N. Yao, *Angew. Chem.* **2008**, *120*, 7411–7415; *Angew. Chem. Int. Ed.* **2008**, *47*, 7301–7305; c) Q. Liao, H. B. Fu, J. N. Yao, *Adv. Mater.* **2009**, *21*, 4153–4157.

[13] P. Jonkheijm, P. Van der Schoot, A. Schenning, E. W. Meijer, *Science* **2006**, *313*, 80 – 83.
[14] V. Bulovic, A. Shoustikov, M. A. Baldo, E. Bose, V. G. Kozlov, M. E. Thompson, S. R. Forrest, *Chem. Phys. Lett.* **1998**, *287*, 455 – 460.
[15] Y. D. Yin, A. P. Alivisatos, *Nature* **2005**, *437*, 664 – 670.
[16] a) B. Mayers, Y. N. Xia, *Adv. Mater.* **2002**, *14*, 279 – 282; b) H. X. Ji, J. S. Hu, Q. X. Tang, W. G. Song, C. R. Wang, W. P. Hu, L. J. Wan, S. T. Lee, *J. Phys. Chem. C* **2007**, *111*, 10498 – 10502.
[17] a) S. M. Yoon, I. C. Hwang, K. S. Kim, H. C. Choi, *Angew. Chem.* **2009**, *121*, 2544 – 2547; *Angew. Chem. Int. Ed.* **2009**, *48*, 2506 – 2509; b) L. W. Yin, Y. Bando, D. Golberg, M. S. Li, *Adv. Mater.* **2004**, *16*, 1833 – 1838.
[18] a) K. Rurack, M. L. Dekhtyar, J. L. Bricks, U. Resch-Genger, W. Rettig, *J. Phys. Chem. A* **1999**, *103*, 9626 – 9635; b) Z. Irena, L. Tali, K. Menahem, *Eur. J. Org. Chem.* **2006**, 4164 – 4169.
[19] Photoisomerization of APO components might alter the local TPI crystalline matrix, thus leading to leakage of guided light, which should be responsible for the selective switch of waveguide to the left tip rather than to the right tip (Figure S14).

